Modelling and Analysis of the Quadrature-booster Phase Shifter with PWM AC Bipolar Matrix-reactance Chopper and Passive Load

Zbigniew FEDYCZAK, Maciej JANKOWSKI, Paweł SZCZEŚNIAK

University of Zielona Góra, Poland

Summary: **This paper deals with a quadrature-booster phase shifter for power flow control and for transient stability improvement in AC transmission systems. The PWM AC bipolar matrix chopper (MC) is proposed for the control of the qudrature voltage component of the original voltage. There are presented in this paper both steady and transient state analyses of a transmission system with passive load based on averaged circuit models. Furthermore, simulation and experimental test results obtained in a three-phase 3 kVA laboratory model are also presented.**

1. INTRODUCTION

The phase control of AC line voltage is one of the well-known methods of power flow control and for transient stability in flexible AC transmission systems (FACTS) [3]. A phase shifter injects a variable voltage with adequate magnitude and phase to shift the phase angle of transmission line phase voltage as shown in Figure 1 [3–6]. Electromechanical or silicon controlled rectifier (SCR) tap-changing transformers are commonly used in conventional realisations of quadrature-booster phase shifters [3, 4]. Regular maintenance of electromechanical tap changers is needed and, furthermore, both electromechanical and SCR ones have relatively slow step response. Generally, solutions of phase shifters with or without the energy storage element are proposed. Phase shifters employing one series connected PWM VSI or two parallel and series connected PWM VSI are proposed in [12]. Because of unlimited phase shifting possibilities (fig. 1b) these topologies can also regulate reactive power in the transmission system. Two types of quadrature phase shifters without energy storage elements (Fig. 1c), employing PWM AC chopper, are presented in [2, 6, 9, 10, 13]. The first type of topology with unipolar PWM AC matrix chopper (MC) has the functional capacity only of injecting unipolar quadrature voltage. The second type with hybrid topology (transformer and MC) has the capacity to inject bipolar quadrature voltage but transformer with two secondary winding and two single-phase MC per phase are used [13]. Furthermore, in the mentioned works only some attention has been dedicated to transient state analysis of the phase shifters.

This paper presents a three-phase quadrature-booster phase shifter with PWM AC bipolar MC, which enables bipolar quadrature voltage injection into the transmission system. The main purpose of this paper is to present averaged circuit models of such phase shifters, which can be used in steady and transient state analysis. This paper is organized as follows: in section 2, the presented phase shifter with switched model of bipolar MC is described; the averaged circuit models both for steady state and for transient state analyses (small signal model) are presented in section 3; in

section 4 some simulation and experimental test results are presented; finally, in section 5, conclusions are provided.

2. DESCRIPTION OF ANALYSED PHASE SHIFTER

The schematic diagram of the proposed three-phase quadrature-booster phase shifter is shown in Figure 2. Input transformers TR_{1a}, TR_{1b} and TR_{1c}, are connected to the line-line supply voltages u_{Scb}, u_{Sac}, u_{Sba} in such manner as to obtain orthogonal compensating voltages u_{Ca}, u_{Cb}, u_{Cc} as shown in Figure 2. Phase MC are used to control the compensating voltages in respective phases. These voltages are fed into the transmission system by a series of connected output transformers TR_{2a}, TR_{2b} and TR_{2c}. Total leakage inductances of the input and the output transformers with capacitors C_{F1a}, C_{F1b}, C_{F1c} and C_{F2a}, C_{F2b}, C_{F2c} are elements of phase MC input and output filters.

Each phase bipolar MC consists of four bi-directional switches (transistors $T_1 - T_8$). The idealised voltage transfer function as a function of pulse duty factor $D = t_1/T_S$ (Table 1) is given by [2]:

$$\frac{U_2}{U_1} = 2D - 1 \qquad (1)$$

The MC substitute schemes, which can be used for detailed description of one operation, are collected in Tab. 1 [2], [1]. In these schemes the wires which conduct the current are shown
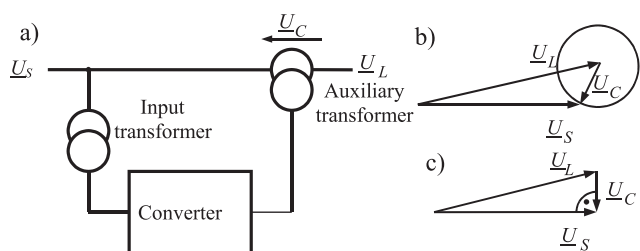

Fig. 1. Phase shifter, a) schematic diagram, b), c) phasors of the phase shifters with and without energy storage element
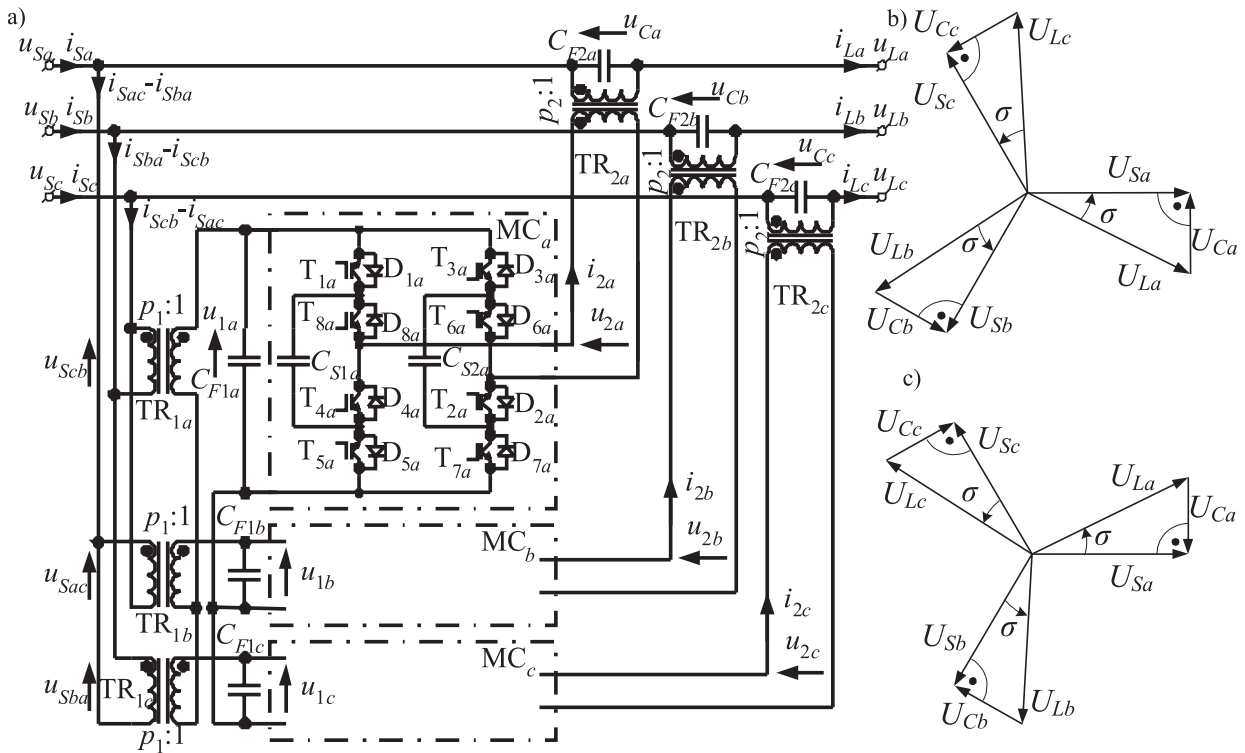
Fig. 2. The quadrature-booster phase shifter with PWM bipolar matrix chopper, a) schematic diagram, b), c) voltage phasors for pulse duty factor $D > 0.5$ and $D < 0.5$ respectively
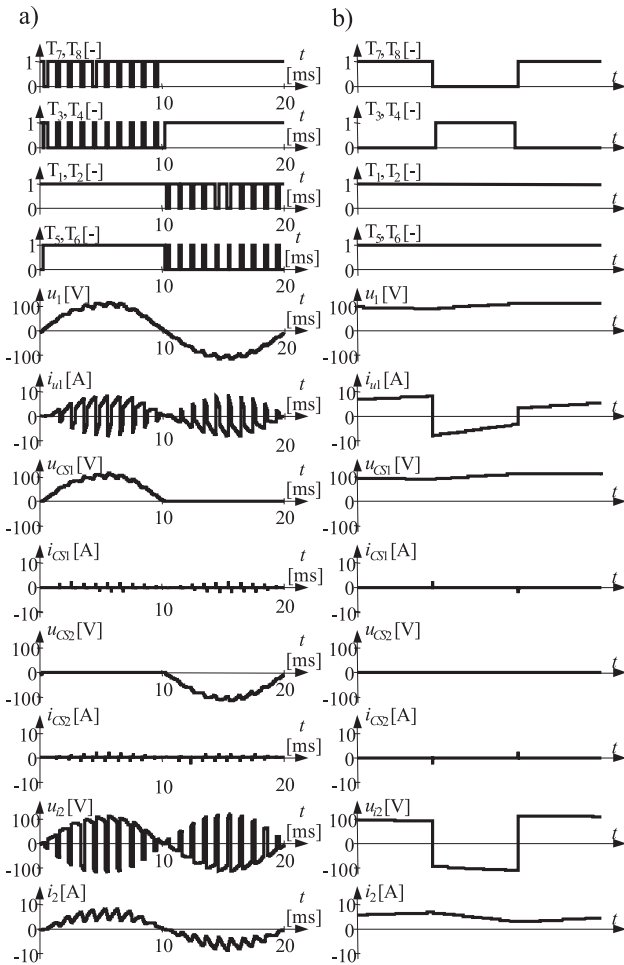

Fig. 3. Exemplary voltage and current time waveforms of the presented MC, a) for supply voltage period T, b) for switching period T_S

by a solid line, whereas the wires which do not conduct the current are shown by a thin solid line. Bypass mode circuits for "dead time" t_D are shown by a dashed line. In the presented solution of the MC a control strategy proposed in [8] is implemented. Exemplary voltage and current time waveforms, both for supply voltage period T and for switching period T_S, which depict the operation of the presented MC, are shown in Figure 3. As is visible (Fig.3) the supplying source current i_{u1} has no overcurrents, and load voltage u_{i2} has no overvoltages. It should be noted that in applied control strategy the snubbed capacitors C_{S1} and C_{S2} are used as overvoltage elements [1, 8].

3. THEORETICAL ANALYSIS

3.1. Steady state modelling

Shown in Figure 4 is a single-phase switched model of the considered phase shifter in a symmetrical transmission system with passive load. In this circuit a MC with ideal bipolar switches is used, where inductors L_{F1} and L_{F2} are the total leakage inductances of the input and output transformers TR_1 and TR_2 respectively. An ideal model of the transformers TR_1 and TR_2 is employed.

Using the average state space method with running switching periods [2, 7], the averaged state space equation (mathematical averaged model) is expressed as:

$$\dot{\mathbf{x}} \approx \mathbf{A}(D)\bar{\mathbf{x}} + \mathbf{B}(D)\mathbf{u}$$

$$\bar{u}_{La} \approx \mathbf{C}(D)\bar{\mathbf{x}} + \mathbf{D}(D)\mathbf{u} \tag{2}$$

Table 1. Substitute schemes of the bipolar MC

where:

$\overline{\mathbf{x}} = \begin{bmatrix} \overline{i}_{1a} & \overline{u}_{1a} & \overline{i}_{3a} & \overline{u}_{Ca} \end{bmatrix}^T$ — vector of the averaged state variables;

$\mathbf{u} = \begin{bmatrix} u_{Sa} & u_{Scb} \end{bmatrix}^T$ — vector of the supply voltages;

$\mathbf{A}(D), \mathbf{B}(D), \mathbf{C}(D), \mathbf{D}(D)$ — averaged state, input, output state and input-output matrixes, which are described as:

$$\mathbf{A}(D) = \begin{bmatrix} 0 & -\dfrac{1}{L_{F1}} & 0 & 0 \\ \dfrac{1}{C_{F1}} & 0 & -\dfrac{(2D-1)}{p_2 C_{F1}} & 0 \\ 0 & \dfrac{(2D-1)}{p_2 L_{F2}} & 0 & -\dfrac{1}{L_{F2}} \\ 0 & 0 & \dfrac{1}{C_{F2}} & -\dfrac{1}{R_L C_{F2}} \end{bmatrix} \quad (3)$$

$$\mathbf{B}(D) = \mathbf{B} = \begin{bmatrix} 0 & \dfrac{1}{p_1 L_{F1}} \\ 0 & 0 \\ 0 & 0 \\ \dfrac{1}{R_L C_{F2}} & 0 \end{bmatrix} \quad (4)$$

$$\mathbf{C}(D) = \mathbf{C} = \begin{bmatrix} 0 & 0 & 0 & -1 \end{bmatrix}$$
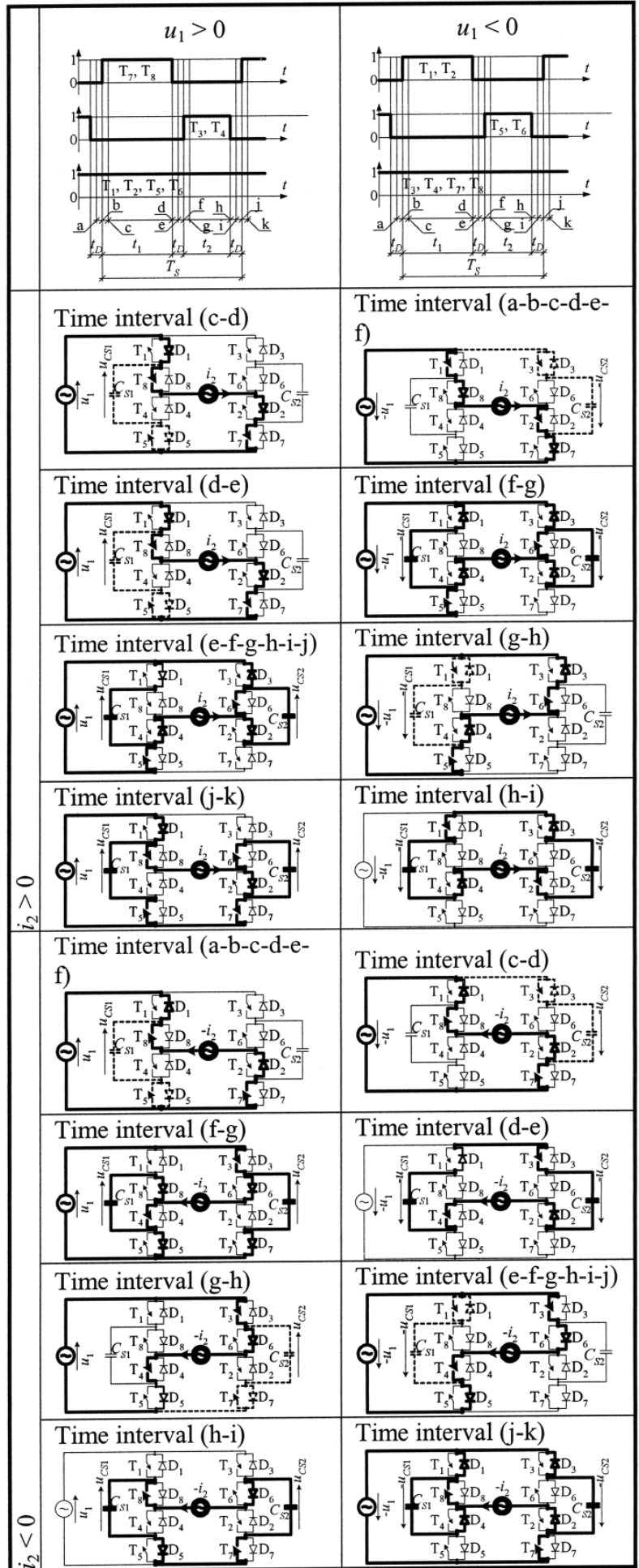$$\mathbf{D}(D) = \mathbf{D} = \begin{bmatrix} 0 & 1 \end{bmatrix} \quad (5)$$

where:
p_1, p_2 — voltage transformation ratios of the TR$_1$ and TR$_2$ transformers.

On the basis of equations (2) – (4) and using an ideal transformer model a single-phase steady-state averaged circuit model can be easily constructed. Such a model for the analysed phase shifter is shown in Figure 5.

In respect to Figure 5, in Figure 6 the substitute schemes for each supply source operated separately are shown.

Referring to Figure 6, allowing for expressions (6, 7) and applying principle of superposition (8, 9) basic steady state properties are described by equations (10–12).

$$\underline{U}_{Scb} = \underline{U}_{Sc} - \underline{U}_{Sb} = \left(a - a^2\right)\underline{U}_{Sa} =$$
$$= j\sqrt{3}\,\underline{U}_{Sa} \quad (6)$$

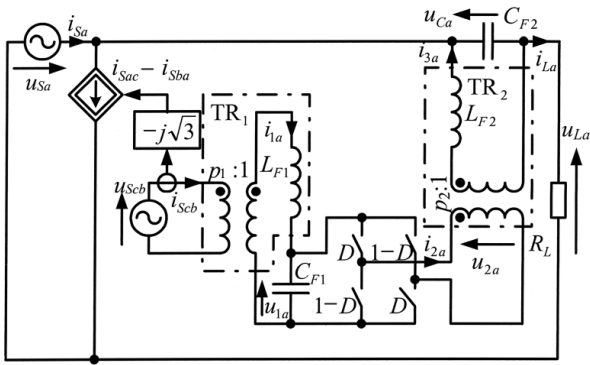|	$u_1 > 0$	$u_1 < 0$
	Time interval (c-d)	Time interval (a-b-c-d-e-f)
$i_2 > 0$	Time interval (d-e)	Time interval (f-g)
	Time interval (e-f-g-h-i-j)	Time interval (g-h)
	Time interval (j-k)	Time interval (h-i)
	Time interval (a-b-c-d-e-f)	Time interval (c-d)
$i_2 < 0$	Time interval (f-g)	Time interval (d-e)
	Time interval (g-h)	Time interval (e-f-g-h-i-j)
	Time interval (h-i)	Time interval (j-k)

Fig. 4. Single-phase switched model of analysed quadrature-booster phase shifter
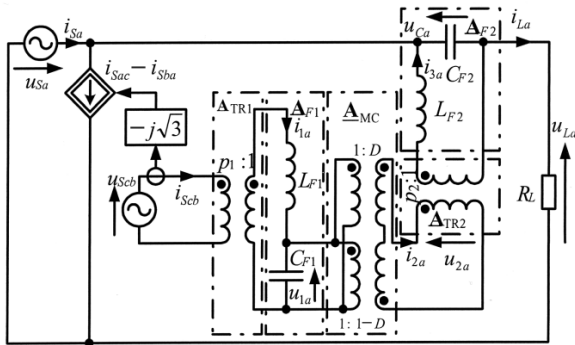

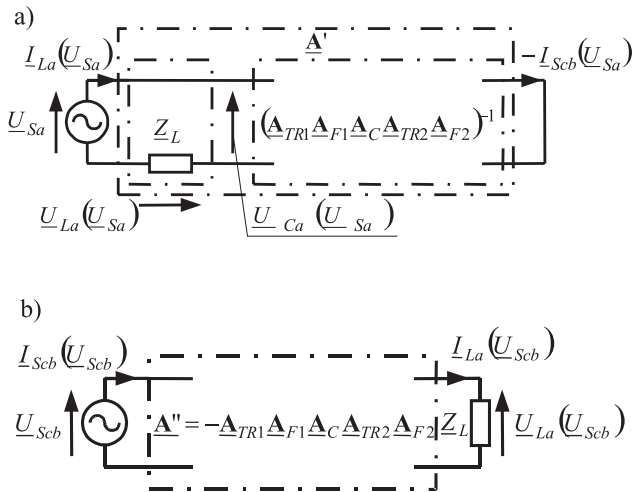Fig. 5. Single-phase steady-state averaged circuit model of analysed phase shifter

a)

b)

Fig. 6. Substitute schemes for a) $\underline{U}_{Scb} = 0$, b) $\underline{U}_{Sa} = 0$

$$\underline{I}_{Sa} = \underline{I}_{La} + \underline{I}_{Sac} - \underline{I}_{Sba} = \underline{I}_{La} + \left(a^2 - a\right)\underline{I}_{Scb} =$$
$$= \underline{I}_{La} - j\sqrt{3}\,\underline{I}_{Scb} \qquad (7)$$

$$\underline{I}_{La} = \underline{I}_{La}\left(\underline{U}_{Sa}\right)\big|_{\underline{U}_{Scb}=0} + \underline{I}_{La}\left(\underline{U}_{Scb}\right)\big|_{\underline{U}_{Sa}=0} \qquad (8)$$

$$\underline{I}_{Scb} = \underline{I}_{Scb}\left(\underline{U}_{Sa}\right)\big|_{\underline{U}_{Scb}=0} + \underline{I}_{Scb}\left(\underline{U}_{Scb}\right)\big|_{\underline{U}_{Sa}=0} \qquad (9)$$

$$\underline{H}_U = \frac{\underline{U}_{La}}{\underline{U}_{Sa}} = \frac{\underline{Z}_L \cdot \underline{I}_{La}}{\underline{U}_{Sa}} \qquad (10)$$

$$\underline{H}_I = \frac{\underline{I}_{La}}{\underline{I}_{Sa}} \qquad (11)$$

$$\lambda_S = cos\left(\varphi_{S1}\right) = cos\left(arg\left(\frac{\underline{U}_{Sa}}{\underline{I}_{Sa}}\right)\right) \qquad (12)$$

where:

$$a = e^{j\frac{2\pi}{3}} = -\frac{1}{2} + j\frac{\sqrt{3}}{2}, \; a^2 = e^{j\frac{4\pi}{3}} = -\frac{1}{2} - j\frac{\sqrt{3}}{2}, \; \underline{H}_U, \underline{H}_I -$$

— voltage and current transmittance;
λ_S — power factor (displacement factor).
Furthermore, the following dependencies should be noted in the calculation of the above expressions:

$$\begin{bmatrix} \underline{U}_{Sa} \\ \underline{I}_{La}\left(\underline{U}_{Sa}\right)\big|_{\underline{U}_{Scb}=0} \end{bmatrix} = \underline{\mathbf{A}}' \begin{bmatrix} 0 \\ -\underline{I}_{Scb}\left(\underline{U}_{Sa}\right)\big|_{\underline{U}_{Scb}=0} \end{bmatrix} \qquad (13)$$

$$\begin{bmatrix} \underline{U}_{Scb} \\ \underline{I}_{Scb}\left(\underline{U}_{Scb}\right)\big|_{\underline{U}_{Sa}=0} \end{bmatrix} = \underline{\mathbf{A}}'' \begin{bmatrix} \underline{U}_{La}\left(\underline{U}_{Scb}\right)\big|_{\underline{U}_{Sa}=0} \\ \underline{I}_{La}\left(\underline{U}_{Scb}\right)\big|_{\underline{U}_{Sa}=0} \end{bmatrix} \qquad (14)$$

where:
four-terminal matrixes (Fig. 6) are expressed by (15) and (16), whereas a detailed description of the component chain parameters is collected in the appendix in Table A1.

$$\underline{\mathbf{A}}' = \begin{bmatrix} 1 & \underline{Z}_L \\ 0 & 1 \end{bmatrix}\left(\underline{\mathbf{A}}_{TR1}\underline{\mathbf{A}}_{F1}\underline{\mathbf{A}}_{MC}\underline{\mathbf{A}}_{TR2}\underline{\mathbf{A}}_{F2}\right)^{-1} \qquad (15)$$

$$\underline{\mathbf{A}}'' = -\underline{\mathbf{A}}_{TR1}\underline{\mathbf{A}}_{F1}\underline{\mathbf{A}}_{MC}\underline{\mathbf{A}}_{TR2}\underline{\mathbf{A}}_{F2} \qquad (16)$$

Exemplary steady state calculation test results of the voltage transmittance and displacement factor of the presented phase shifter, for purposes of comparison, are collected together with simulation and experimental results and are shown in Figures 9 and 10.

3.2. Small signal model

Assuming that all variables have two components: a running constant component (the averaged value in the switching period T_S), which is marked by upper case letter, and a perturbation one marked by lower case letter, which is covered by sign "^":

$$\mathbf{u} = \mathbf{U} + \hat{\mathbf{u}}, \; \mathbf{x} = \mathbf{X} + \hat{\mathbf{x}}, \; u_{La} = U_{La} + \hat{u}_{La} \; \text{ and } \; d = D + \hat{d} \quad (17)$$

On the basis of the averaged state space method the small signal state space equations are expressed as follow [11]:

$$\frac{d}{dt}(\mathbf{X}+\hat{\mathbf{x}}) \approx \mathbf{A}\hat{\mathbf{x}}+\mathbf{B}\hat{\mathbf{u}}+\left[(\mathbf{A}_1-\mathbf{A}_2)\mathbf{X}+(\mathbf{B}_1-\mathbf{B}_2)\mathbf{U}\right]\hat{d}$$

$$U_{La}+\hat{u}_{La}=\mathbf{C}\hat{\mathbf{x}}+\mathbf{D}\hat{\mathbf{u}} \tag{18}$$

where:

$$\mathbf{A}_1(D)=\mathbf{A}(D)-\mathbf{A}_2(D)$$
$$\mathbf{B}_1(D)=\mathbf{B}(D)-\mathbf{B}_2(D)$$

With reference to (18) complete steady state and small signal description is expressed by (19–23).

For i_{1a}:

$$\frac{d}{dt}\left(I_{1a}+\hat{i}_{1a}\right)=-\frac{1}{L_{F1}}\left(U_{1a}+\hat{u}_{1a}\right)+\frac{1}{p_1 L_{F1}}\left(U_{Scb}+\hat{u}_{Scb}\right) \tag{19}$$

for u_{1a}:

$$\tag{20}$$

$$\frac{d}{dt}\left(U_{1a}+\hat{u}_{1a}\right)=\frac{1}{C_{F1}}\left(I_{1a}+\hat{i}_{1a}\right)-\frac{2(D+\hat{d})-1}{p_2 C_{F1}}\left(I_{3a}+\hat{i}_{3a}\right)=$$

$$=\frac{1}{C_{F1}}\left(I_{1a}+\hat{i}_{1a}\right)-\frac{2D-1}{p_2 C_{F1}}\left(I_{3a}+\hat{i}_{3a}\right)-\frac{2\hat{d}}{p_2 C_{F1}}I_{3a}-\underbrace{\frac{2\hat{d}}{p_2 C_{F1}}\hat{i}_{3a}}_{\text{nonlinear term}}$$

for i_{3a}:

$$\tag{21}$$

$$\frac{d}{dt}\left(I_{3a}+\hat{i}_{3a}\right)=\frac{2(D+\hat{d})-1}{p_2 L_{F2}}\left(U_{1a}+\hat{u}_{1a}\right)-\frac{1}{L_{F2}}\left(U_{Ca}+\hat{u}_{Ca}\right)=$$

$$=\frac{2D-1}{p_2 L_{F2}}\left(U_{1a}+\hat{u}_{1a}\right)+\frac{2\hat{d}}{p_2 L_{F2}}U_{1a}+\underbrace{\frac{2\hat{d}}{p_2 L_{F2}}\hat{u}_{1a}}_{\text{nonlinear term}}-\frac{1}{L_{F2}}\left(U_{Ca}+\hat{u}_{Ca}\right)$$

for u_{Ca}:

$$\frac{d}{dt}\left(U_{Ca}+\hat{u}_{Ca}\right)=\frac{1}{C_{F2}}\left(I_{3a}+\hat{i}_{3a}\right)-$$

$$-\frac{1}{R_L C_{F2}}\left(U_{Ca}+\hat{u}_{Ca}\right)+\frac{1}{R_L C_{F2}}\left(U_{Sa}+\hat{u}_{Sa}\right) \tag{22}$$

and for u_{La} (output equation):

$$\left(U_{La}+\hat{u}_{La}\right)=-\left(U_{Ca}+\hat{u}_{Ca}\right)+\left(U_{Sa}+\hat{u}_{Sa}\right) \tag{23}$$

A complete single-phase steady state and small signal averaged circuit model (canonical averaged model) constructed from equations (18–23) is shown in Figure 7.

According to equations (18–22) and with reference to Figure 7 additional voltage and current controlled sources $e(\hat{d})$ (24) and $j(\hat{d})$ (25) should be allowed during small signal analysis.

$$j_a\left(\hat{d}\right)=\frac{2I_{3a}}{p_2}\hat{d} \quad (24) \qquad e_a\left(\hat{d}\right)=\frac{2U_{1a}}{p_2}\hat{d} \quad (25)$$

According to (18) a Laplace transform of a small signal state space averaged model is expressed as:

$$s\hat{\mathbf{x}}(s)=\mathbf{A}\hat{\mathbf{x}}(s)+\mathbf{B}\hat{\mathbf{u}}(s)+\left[(\mathbf{A}_1-\mathbf{A}_2)\mathbf{X}+(\mathbf{B}_1-\mathbf{B}_2)\mathbf{U}\right]\hat{d}(s)$$

$$\hat{u}_{La}(s)=\mathbf{C}\hat{\mathbf{x}}(s)+\mathbf{D}\hat{\mathbf{u}}(s) \tag{26}$$

solutions of these equations in complex form:

$$\hat{\mathbf{x}}(s)=(s\mathbf{I}-\mathbf{A})^{-1}\left\{\mathbf{B}\hat{\mathbf{u}}(s)+\left[(\mathbf{A}_1-\mathbf{A}_2)\mathbf{X}+(\mathbf{B}_1-\mathbf{B}_2)\mathbf{U}\right]\hat{d}(s)\right\}=$$

$$=\mathbf{G}_{\hat{\mathbf{x}},\hat{\mathbf{u}}}(s)\hat{\mathbf{u}}(s)+\mathbf{G}_{\hat{\mathbf{x}},\hat{d}}(s)\hat{d}(s) \tag{27}$$
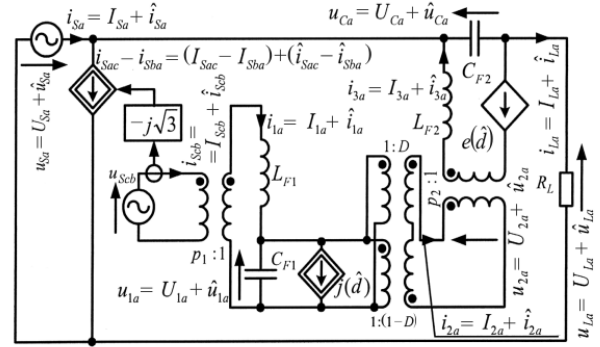

Fig. 7. Complete single-phase steady state and small signal averaged circuit model of analysed quadrature phase shifter
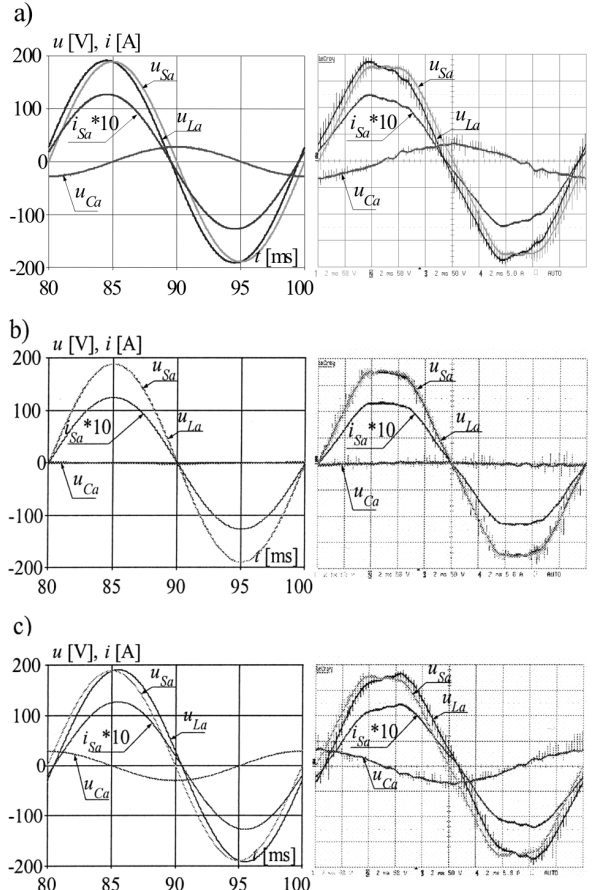

Fig. 8. Exemplary simulation and experimental voltage and current time waveforms for a) $D = 0.1$, b) $D = 0.5$, b) $D = 0.9$

Table 2. Small signal transfer functions of analysed quadrature phase shifter.

$$\mathbf{G}_{\hat{\mathbf{x}},\hat{\mathbf{u}}}(s) = \frac{\hat{\mathbf{x}}(s)}{\hat{\mathbf{u}}(s)} =$$

$$= \frac{\begin{bmatrix} -\dfrac{1}{R_L L_{F1} L_{F2} C_{F1} C_{F2} P} & \dfrac{1}{p_1 L_{F1}} s^3 + \dfrac{1}{p_1 R_L L_{F1} C_{F2}} s^2 + \dfrac{C_{F1} P^2 + C_{F2}}{p_1 L_{F1} L_{F2} C_{F1} C_{F2} P^2} s + \dfrac{1}{p_1 R_L L_{F1} L_{F2} C_{F1} C_{F2} P^2} \\[3mm] \dfrac{1}{R_L L_{F2} C_{F1} C_{F2} P} s & \dfrac{1}{p_1 L_{F1} C_{F1}} s^2 + \dfrac{1}{p_1 R_L L_{F1} C_{F1} C_{F2}} s + \dfrac{1}{p_1 L_{F1} L_{F2} C_{F1} C_{F2}} \\[3mm] -\dfrac{1}{R_L L_{F2} C_{F2}} s^2 - \dfrac{1}{R_L L_{F1} L_{F2} C_{F1} C_{F2}} & \dfrac{1}{p_1 L_{F1} L_{F2} C_{F2} P} s + \dfrac{1}{p_1 R_L L_{F1} L_{F2} C_{F1} C_{F2} P} \\[3mm] \dfrac{1}{R_L C_{F2}} s^3 + \dfrac{L_{F2} P^2 + L_{F1}}{R_L L_{F1} L_{F2} C_{F1} C_{F2} P^2} & \dfrac{1}{p_1 L_{F1} L_{F2} C_{F1} C_{F2} P} \end{bmatrix}}{det(s\mathbf{I} - \mathbf{A})}$$

$$\mathbf{G}_{\hat{\mathbf{x}},\hat{d}}(s) = \frac{\hat{\mathbf{x}}(s)}{\hat{d}(s)} =$$

$$= \frac{\begin{bmatrix} -\dfrac{2}{p_2 R_L L_{F1} C_{F1}} s^2 - \dfrac{2}{p_2 R_L^2 L_{F1} C_{F2}} s - \dfrac{2}{p_2 R_L L_{F2} C_{F1} C_{F2}} & \dfrac{2}{p_1 p_2 R_L L_{F1} C_{F1} P} s^2 + \dfrac{2(R_L^2 C_{F2} + L_{F2})}{p_1 p_2 R_L^2 L_{F1} L_{F2} C_{F1} C_{F2} P} s + \dfrac{4}{p_1 p_2 R_L L_{F1} C_{F1} C_{F2}} \\[3mm] \dfrac{2}{p_2 R_L C_{F1}} s^3 + \dfrac{2}{p_2 R_L^2 C_{F1} C_{F2}} s^2 + \dfrac{2}{p_2 R_L L_{F2} C_{F1} C_{F2}} s & -\dfrac{2}{p_1 p_2 R_L C_{F1} P} s^3 - \dfrac{2(R_L^2 C_{F2} + L_{F2})}{p_1 p_2 R_L^2 L_{F2} C_{F1} C_{F2} P} s^2 - \dfrac{4}{p_1 p_2 R_L L_{F2} C_{F1} C_{F2} P} s \\[3mm] \dfrac{2}{p_2 R_L C_{F1} L_{F2} P} s^2 + \dfrac{2}{p_2 R_L^2 L_{F2} C_{F1} C_{F2} P} s & \dfrac{2}{p_1 p_2 L_{F2}} s^3 + \dfrac{2(C_{F1} P^2 - C_{F2})}{p_1 p_2 R_L L_{F2} C_{F1} C_{F2} P^2} s^2 + \dfrac{2(R_L^2 C_{F2} P^2 - L_{F1})}{p_1 p_2 R_L^2 L_{F1} L_{F2} C_{F1} C_{F2} P^2} s + \dfrac{2}{p_1 p_2 R_L L_{F1} L_{F2} C_{F1} C_{F2}} \\[3mm] \dfrac{2}{p_2 R_L L_{F2} C_{F1} C_{F2} P} s & \dfrac{2}{p_1 p_2 L_{F2} C_{F2}} s^2 - \dfrac{2}{p_1 p_2 R_L L_{F2} C_{F1} C_{F2} P^2} s + \dfrac{2}{p_1 p_2 L_{F1} L_{F2} C_{F1} C_{F2}} \end{bmatrix} \mathbf{U}}{det(s\mathbf{I} - \mathbf{A})}$$

$$G_{\hat{u}_{La},\hat{\mathbf{u}}}(s) = \frac{\hat{u}_{La}(s)}{\hat{\mathbf{u}}(s)} =$$

$$= \frac{\begin{bmatrix} \dfrac{(L_{F1} C_{F1} + L_{F2} C_{F2}) P^2 + L_{F1} C_{F2}}{L_{F1} L_{F2} C_{F1} C_{F2} P^2} s^2 + \dfrac{L_{F2} P^2 + L_{F1}}{R_L L_{F1} L_{F2} C_{F1} C_{F2} P^2} & + \dfrac{1}{L_{F1} L_{F2} C_{F1} C_{F2}} \end{bmatrix}}{det(s\mathbf{I} - \mathbf{A})}$$

$$G_{\hat{u}_{La},\hat{d}}(s) = \frac{\hat{u}_{La}(s)}{\hat{d}(s)} =$$

$$= \frac{\begin{bmatrix} -\dfrac{2}{p_2 R_L L_{F2} C_{F1} C_{F2} P} s & -\dfrac{2}{p_1 p_2 L_{F2} C_{F2}} s^2 + \dfrac{2}{p_1 p_2 R_L L_{F2} C_{F1} C_{F2} P^2} s - \dfrac{2}{p_1 p_2 L_{F1} L_{F2} C_{F1} C_{F2}} \end{bmatrix} \mathbf{U}}{det(s\mathbf{I} - \mathbf{A})}$$

$$det(s\mathbf{I} - \mathbf{A}) =$$

$$= s^4 + \dfrac{1}{R_L C_{F2}} s^3 + \dfrac{(L_{F1} C_{F1} + L_{F2} C_{F2}) P^2 + L_{F1} C_{F2}}{L_{F1} L_{F2} C_{F1} C_{F2} P^2} s^2 + \dfrac{L_{F2} P^2 + L_{F1}}{R_L L_{F1} L_{F2} C_{F1} C_{F2} P^2} s + \dfrac{1}{L_{F1} L_{F2} C_{F1} C_{F2}}$$

$$\hat{u}_{La}(s) = \left[\mathbf{C} \cdot \mathbf{G}_{\hat{\mathbf{x}},\hat{\mathbf{u}}}(s) + \mathbf{D}\right] \hat{\mathbf{u}}(s) + \left[\mathbf{C} \cdot \mathbf{G}_{\hat{\mathbf{x}},\hat{d}}(s)\right] \hat{d}(s) =$$
$$= \mathbf{G}_{\hat{u}_{La},\hat{\mathbf{u}}}(s) \cdot \hat{\mathbf{u}}(s) + G_{\hat{u}_{La},\hat{d}}(s) \cdot \hat{d}(s) \qquad (28)$$

where:

$$\mathbf{G}_{\hat{x},\hat{u}}(s) = \frac{\hat{\mathbf{x}}(s)}{\hat{\mathbf{u}}(s)} \qquad (28)$$

$$G_{\hat{x},\hat{d}}(s) = \frac{\hat{x}(s)}{\hat{d}(s)} \qquad (29)$$

and:

$$G_{\hat{u}_{La},\hat{\mathbf{u}}}(s) = \frac{\hat{u}_{La}(s)}{\hat{\mathbf{u}}(s)} \qquad (30)$$

$$G_{\hat{u}_{La},\hat{d}}(s) = \frac{\hat{u}_{La}(s)}{\hat{d}(s)} \qquad (30)$$

are the transfer functions, which describe dynamical input-state, control-state, input-output and control-output properties of analysed phase shifter. These dependencies are collected in Table 2.

4. SIMULATION AND EXPERIMENTAL TEST RESULTS

In order to confirm the theoretical approach, simulation and experimental investigations of the analysed solution have been made. The switched model scheme used during simulation tests is shown in Figure 4, however, the laboratory model scheme used during experimental tests is shown in Figure 2. The values of the relevant circuit parameters are collected in appendix Table A2.

In Figures 8–10 exemplary time waveforms and basic property characteristics are shown to illustrate the analysed phase shifter steady state operation.

As can be seen in Figure 8 the phase shifter output voltage u_{La} for $D < 0.5$ is shifted in phase with positive angle (leaded phase) to input voltage, for $D > 0.5$ it is shifted in negative phase (lagged phase). For $D = 0.5$ the output voltage is in phase with input voltage. The same is confirmed by characteristics in Figure 9. It should be noted that changing the load voltage phase does not influence the input displacement factor of the phase shifter (Fig. 10).

The calculation and simulation (PSpice) test results of transient states for the the analysed phase shifter are illustrated in the following figures, from Figures 11 to 22. In the first part, in figures from Figures 11 to 16, transient states are presented at the step change of the input voltages u_{Sa} and u_{Scb} from 100% to 75 % of their nominal values in time moment t_0 and with the pulse duty factor $d = D = 0.75$.
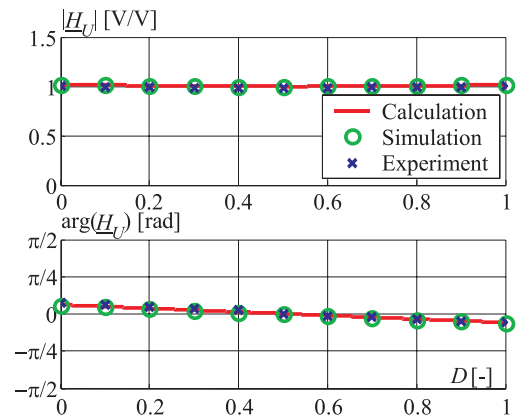

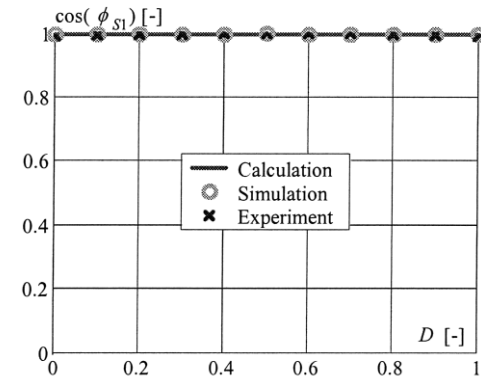Fig. 9. Magnitude and phase of the voltage transmittance as a function of pulse duty factor D

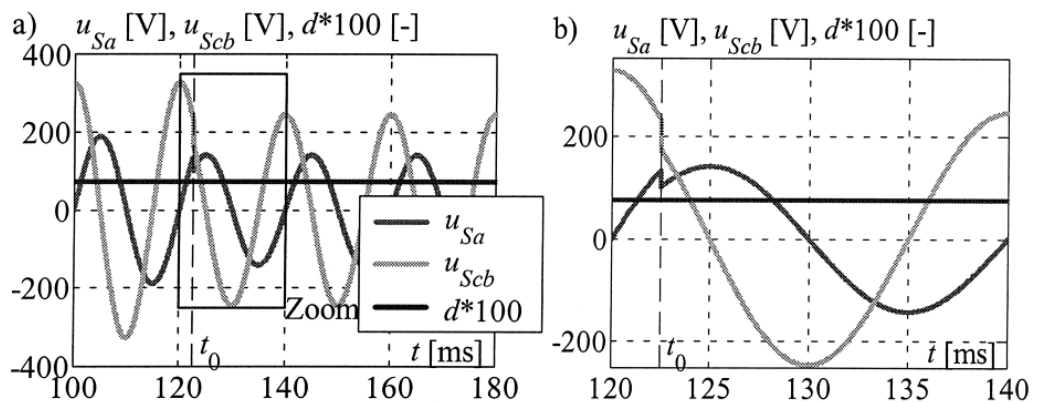Fig. 10. Input displacement factor as a function of pulse duty factor D

Fig. 11. Input voltage time waveforms for transient state where $D = 0.75$,
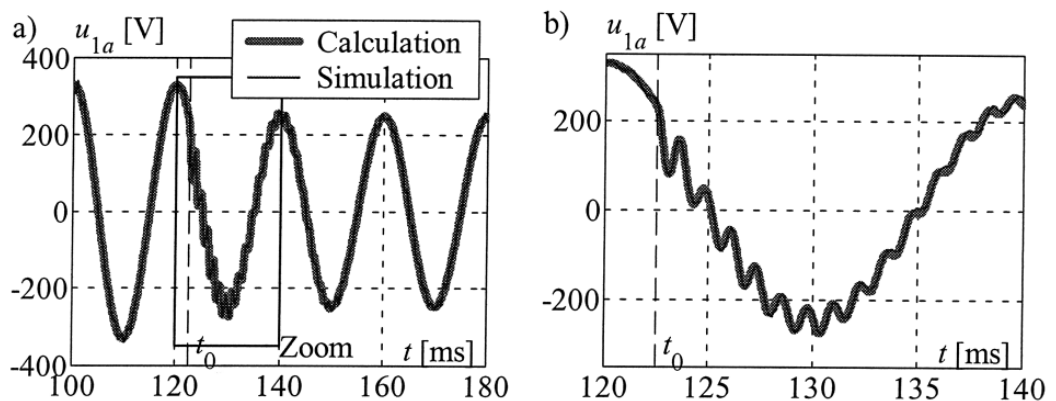a) analysed period,
b) zoom

Fig. 12. MC input voltage time waveforms for step change of the supply voltage where $D = 0.75$,
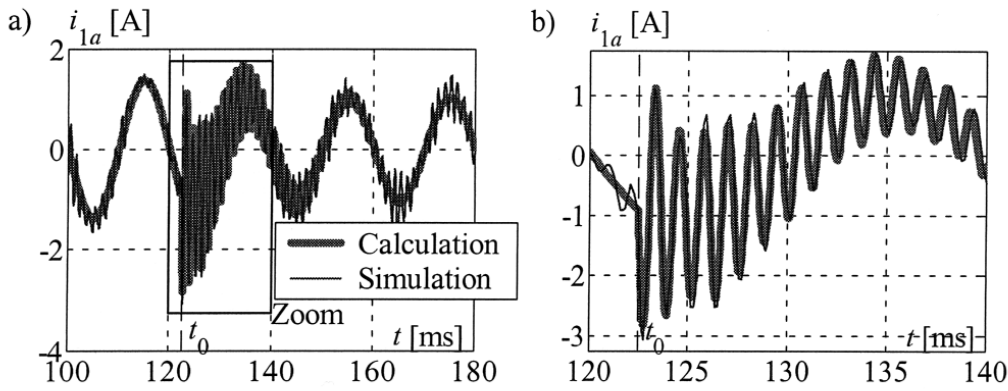a) analysed period,
b) zoom

Fig. 13. MC input current time waveforms for step change of the supply voltage where $D = 0.75$, a) analysed period, b) zoom
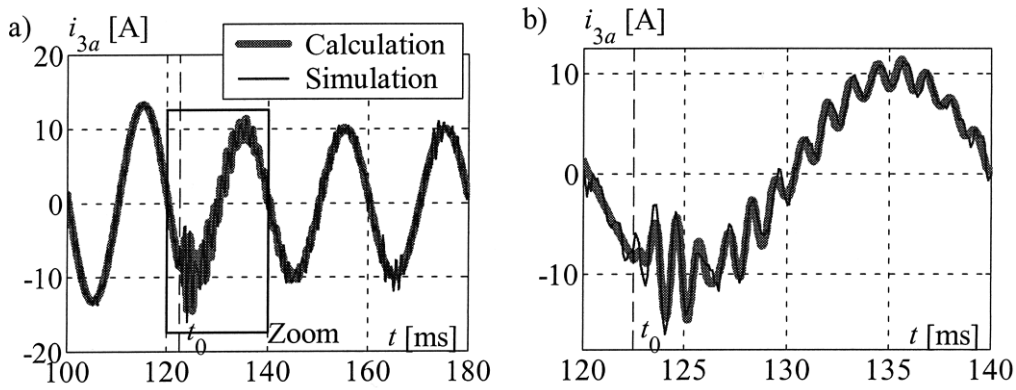

Fig. 14. MC output current time waveforms for step change of the supply voltage where $D = 0.75$, a) analysed period, b) zoom
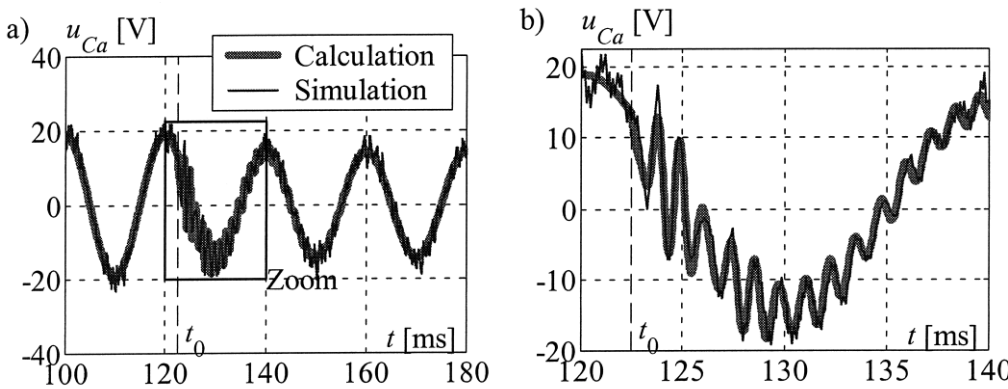

Fig. 15. Compensating voltage time waveforms for step change of the supply voltage where $D = 0.75$, a) analysed period, b) zoom
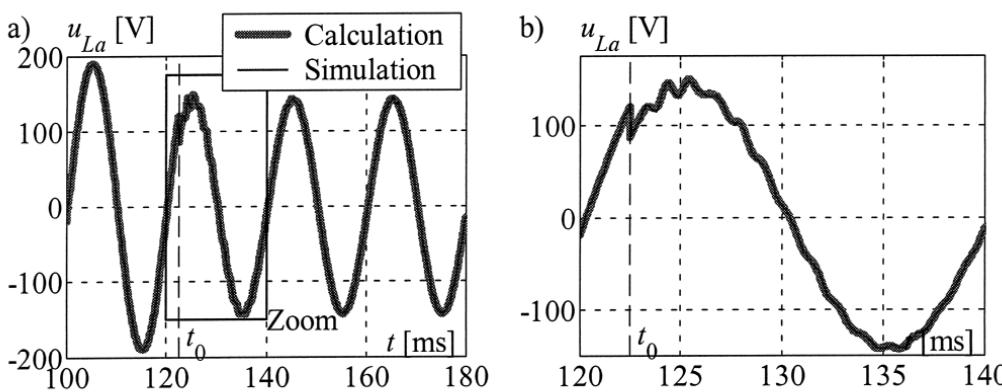

Fig. 16. Load voltage time waveforms for step change of the supply voltage where $D = 0.75$, a) analysed period, b) zoom

Fig. 17. Supply voltage time waveforms for step change of d from 0.25 to 0.75 for nominal values of input voltages, a) analysed period, b) zoom
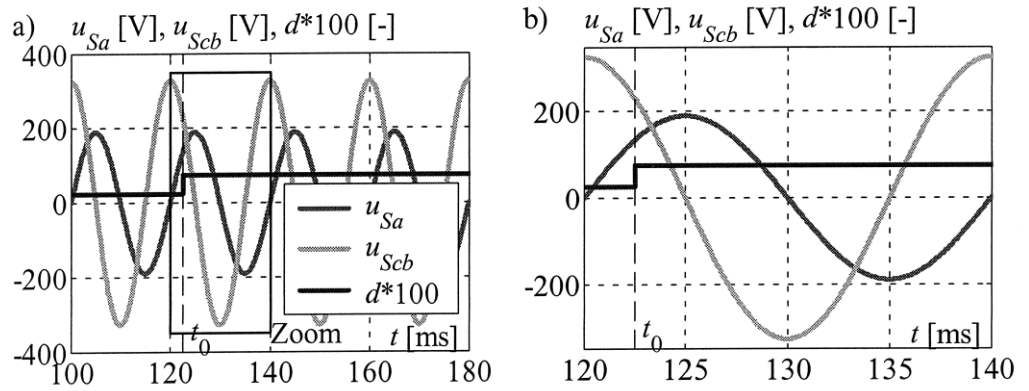

Fig. 18. MC input voltage time waveforms for step change of d from 0.25 to 0.75 for nominal value of supply voltage, a) analysed period, b) zoom
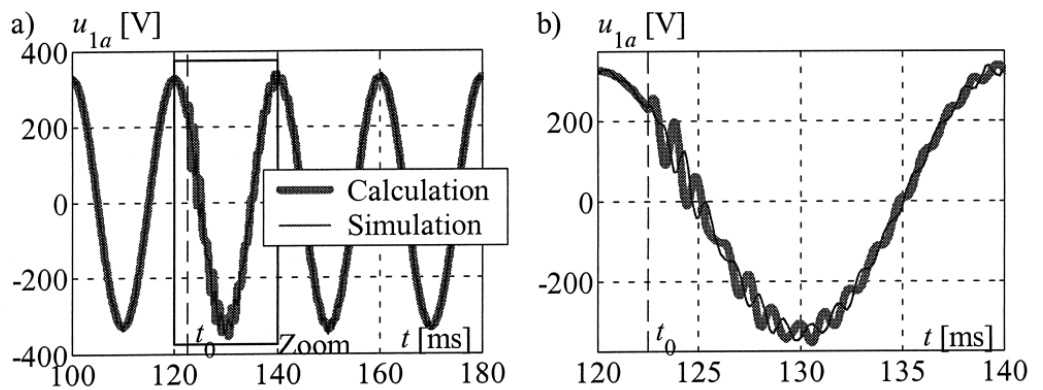

Fig. 19. MC input current time waveforms for step change of d from 0.25 to 0.75 for nominal value of supply voltage, a) analysed period, b) zoom
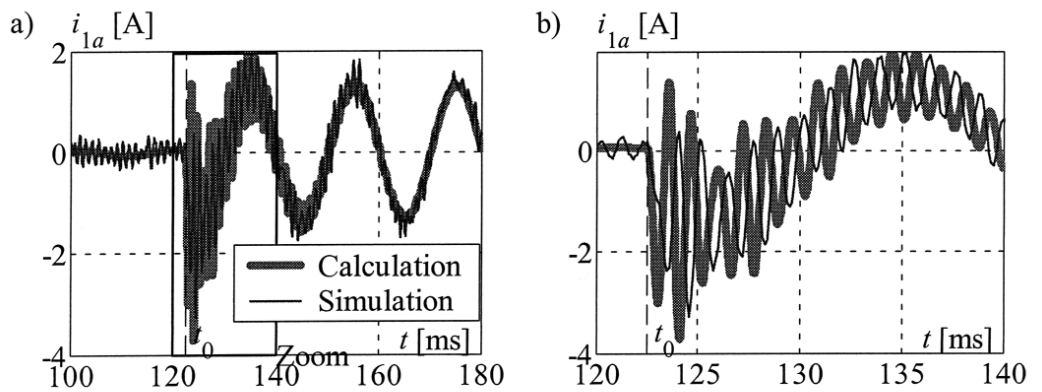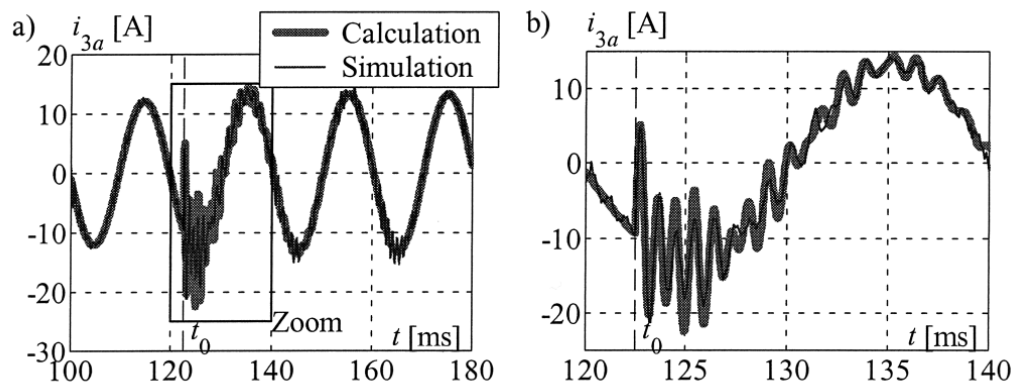

Fig. 20. MC output current time waveforms for step change of d from 0.25 to 0.75 for nominal value of supply voltage, a) analysed period, b) zoom
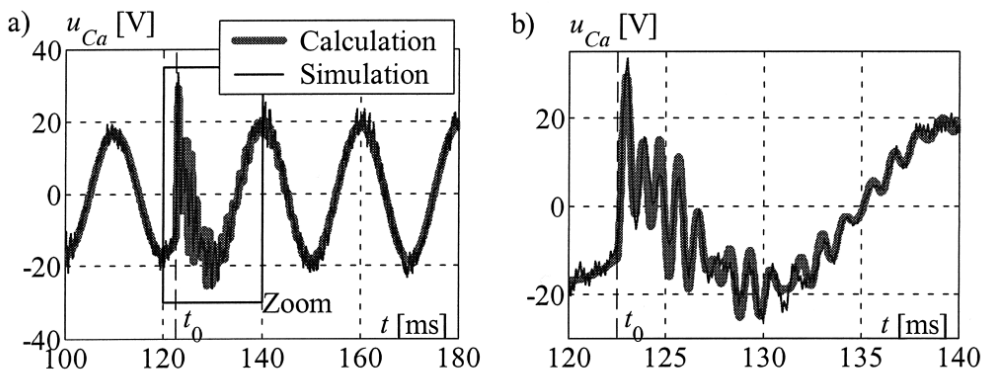
Fig. 21. Compensating voltage time waveforms for step change of d from 0.25 to 0.75 for nominal value of supply voltage,
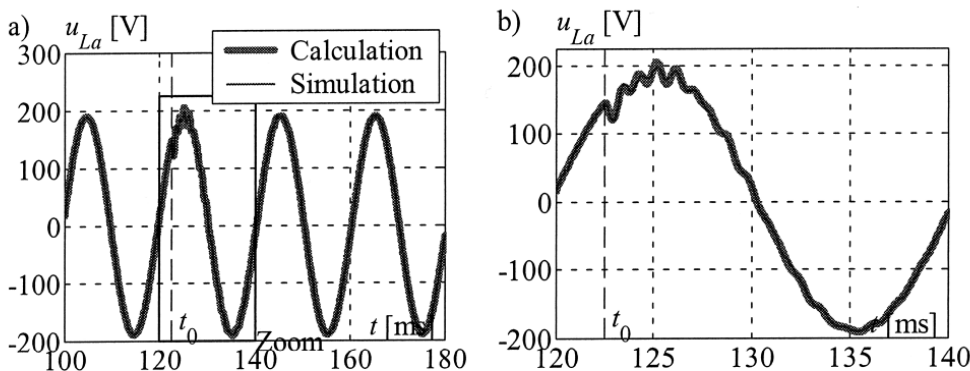a) analysed period,
b) zoom

Fig. 22. Load voltage time waveforms for step change of d from 0.25 to 0.75 for nominal value of supply voltage,
a) analysed period,
b) zoom

Figures from Figure 12 to 16 show good consistency of calculation and simulation test results. Furthermore, they illustrate that parameters of the MC input and output filters should be corrected in order to decrease the oscillation period, especially of the compensating voltage u_C at step change of the supply voltage.

In the second part of the research results, presented in figures from Figure 17 to 22, there are transient states at step changes of impulse duty factor d from 0.25 to 0.75 for nominal values of input voltages, as shown in Figure 17.

Figures from Figure 18 to 22 also show good consistency in calculation and simulation test results of properties connected with the output-control signal transmittance. The obtained results confirm that the small signal averaged (mathematical and circuit) models presented in section 3 can be useful in transient responses analysis of the described phase shifter. In the analysed circuit the response time for step change of d from 0.25 to 0.75 is less than a half period of supply voltage. Similarly to properties connected with output-supply voltage transmittance, optimisation of MC input and output filter parameters should also be continued.

5. CONCLUSIONS

The steady state and small signal averaged mathematical and circuit models of quadrature-booster phase shifter with bipolar MC and passive load have been elaborated. Furthermore, the steady state characteristics and transient responses of the analysed phase shifter have also been investigated. Both simulation test results, obtained for one phase shifter with MC switched model (non-stationary circuit), and experimental ones have confirmed that elaborated models can be useful in steady state and transient responses of the analysed phase shifter. In the analysed circuit the response time for step change of d from 0.25 to 0.75 is less than a half period of supply voltage. These investigations also show that optimisation of MC input and output filter parameters should also be continued, especially in order to decrease the oscillation period of the compensating voltage u_C at both the step changes of the control signal and supply voltage as well. The validity of the proposed models will be the subject of future investigations of the presented phase shifter with active load and for closed control systems as well.

6. APPENDIX

Table A1 shows parameters of the chain matrixes and Table A2 shows simulation and experimental test circuit parameters.

REFERENCES

1. F e d y c z a k Z . , J a n k o w s k i M . , S z c z e ś n i a k P . : *A comparison of basic properties of single-phase serial AC voltage controllers using bipolar chopper.* Proc. of 11th EPE conf. Dresden 2005.
2. F e d y c z a k Z .: *PWM AC voltage transforming circuits.* (In Polish). Oficyna Wydawnicza Uniwersytetu Zielonogórskiego 2003.
3. H i n g o r a n i N . G . , G y u g y i L .: *Understanding FACTS.* IEEE Press, New York 1999.

Table A1. Parameters of the chain matrixes.

Parameter	Matrix description
$\underline{A}_{TR1,2}$	$\begin{bmatrix} p_{1,2} & 0 \\ 0 & 1/p_{1,2} \end{bmatrix}$
$\underline{A}_{MC}$	$\begin{bmatrix} 1/(2D-1) & 0 \\ 0 & 2D-1 \end{bmatrix}$
$\underline{A}_{F1,2}$	$\begin{bmatrix} 1-\omega^2 L_{F1,2} C_{F1,2} & j\omega L_{F1,2} \\ j\omega C_{F1,2} & 1 \end{bmatrix}$

Table A2. Simulation and experimental test circuit parameters.

Parameter	Symbol	Value
Supply voltage, frequency	U_S, f	133/230 V, 50 Hz
Switching frequency	f_S	5 kHz
Filter inductances	L_{F1}, L_{F2}	5.4 mH, 0.238 mH
Filter capacitances	C_{F1}, C_{F2}	6.2 μF, 100 μF
Load resistance	R_L	15 Ω
Transformation ratios	p_1, p_2	230/230 V/V
		230/24 V/V

4. Irvani M.R., Maratukulam D.: *Rewiev of semiconductor-controlled (static) phase shifters for power system applications*. IEEE Trans. on Power Systems Vol. 9, No. 4, pp. 1833–1839. Nov. 1994.
5. Jiang F., Choi S.S., Shrestha G.: *Power system stability enhancement using static phase shifter*. IEEE Trans. on Power Electronics. Vol. 12, No. 1, pp. 207–214. Febr. 1997.
6. Jonson B.K., Venkataramanan G.: *A hybrid PWM solid state phase shifter using PWM AC converters*. IEEE Trans. on Power Delivery Vol. 13, No. 4, pp. 1316–1321. Oct. 1998.
7. Korotyeyev I.Y., Fedyczak Z.: *Steady-state modelling of basic unipolar PWM AC line matrix-reactance choppers*. The Int. Journal for Comp. and Mat. in Electrical and Electronic Eng., COMPEL, Vol. 24 No. 1, 2005, pp. 55–68.
8. Lefeuvre E., Meynard T., Viarouge P.: *Robust two-level and multilevel PWM AC choppers*. Proc. of 9th EPE conf., CD, DS.1-23, P.1-P.8. Graz 2001.
9. Lopez L.A.C., Joos G., Ooi B-T.: *A PWM quadrature-booster phase shifter for FACTS*. IEEE Trans. on Power Delivery Vol. 11, No. 4, pp. 1999–2004. Oct. 1996.
10. Lopez L.A.C., Joos G., Ooi B-T.: *A PWM quadrature-booster phase shifter for AC power transmission*. IEEE Trans. on Power Electronics. Vol. 12, No. 1, pp. 138–143. Jan. 1997.
11. Middlebrock R.D., Ćuk S. *A general unified approach to modelling switching-converter power stages*. Proc. of PESC'76, pp. 18–34. 1976.
12. Ooi B.T., Dal S.Z. Gallana F.D.: *A solid state PWM phase shifter*. IEEE Trans. on Power Electronics. Vol. 8, No. 2, pp. 573 – 579. Apr. 1993.
13. Uemura S., Arimitsu M., Chikaraishi H., Shimada R.: *Active power filter using solid state phase shifter*. Proc. of EPE conf., pp. 185–190. Brighton 1993,.

Zbigniew Fedyczak
was born in Zielona Góra, Poland, in 1952. He graduated from The Higher School of Engineering in Zielona Góra (now The University of Zielona Góra), Poland, in 1976 and 1982 with the degrees of B.S. and M.Sc. respectively in automation and metrology. He was awarded the degree of Ph.D. (with honours) in electrical engineering by the Warsaw Technical University, Warsaw, Poland in 1996, and a Dr. Sc., by Zielona Góra University, Poland in 2004. He worked at LUMEL, Zielona Góra, Poland, as a Design Engineer, from April 1983 to October 1992, where he was involved in the AC/AC thyristor controller design program. He joined the Institute of Electrical Engineering at The University of Zielona Góra, Poland in 1992, where he is an Associate Professor. His research interests include power electronics AC/AC transforming circuits, especially topology and modelling of PWM AC line matrix and matrix-reactance choppers, matrix converters and direct AC/AC frequency converters. He is the author or co-author of more then 70 periodical and conference papers and 10 patents. He is a member of IEEE and EPE.
Address:
University of Zielona Góra, Institute of Electrical Engineering, ul. Podgórna 50, 65-246, Zielona Góra, Poland, e-mail: Z.Fedyczak@iee.uz.zgora.pl,

Maciej Jankowski
was born in Zielona Góra, Poland, in 1976. He graduated from The University of Zielona Góra in 2002, with the degree of M.Sc., majoring in automation in power electrics. Following this, in the same year, he started Postgraduate Studies at The University of Zielona Góra on a course of Electrical Engineering. Since March 2003 Maciej Jankowski has been an assistant in the Institute of Electrical Engineering at The University of Zielona Góra. His research interests include power electronics AC/AC transforming circuits, especially topology and modelling of PWM AC line matrix and matrix-reactance choppers. He is the author or co-author of 6 conference papers.
Address:
University of Zielona Góra, Institute of Electrical Engineering, ul. Podgórna 50, 65-246, Zielona Góra, Poland, e-mail: M.Jankowski@iee.uz.zgora.pl

Paweł Szcześniak
was born in 1979 in Krosno Odrzańskie, Poland. He received the degree of M.Sc. in electrical engineering from The University of Zielona Góra. At present he is Assistant Professor in the Institute of Electrical Engineering at The University of Zielona Góra. His field of interest is matrix converters and matrix - reactance frequency converters. He is the author or co-author of 6 conference papers.
Address:
University of Zielona Góra, Institute of Electrical Engineering, ul. Podgórna 50, 65-246, Zielona Góra, Poland, e-mail: P.Szczesniak@iee.uz.zgora.pl